Second Conference on Smart Monitoring,
Assessment and Rehabilitation of Civil Structures

SMAR 2013

Behavior of FRP-Reinforced Concrete Slabs under Temperature and Sustained Load Effects

H. Bellakehal[1,2], A. Zaidi[1], and R. Masmoudi[2]

[1]Structures Rehabilitation and Materials Laboratory, Laghouat University, Laghouat, Algeria
[2]Department of Civil Engineering, University of Sherbrooke, Sherbrooke, Qc, Canada

ABSTRACT: The large temperature variation has a harmful effect on concrete structures reinforced with fiber reinforced polymer (FRP) bars. This is due to the significant difference between transverse coefficient of thermal expansion of these bars and that of the hardened concrete. This difference generates a radial pressure at the FRP bar/concrete interface, and induces splitting cracks within concrete. This paper presents an analytical study of FRP-reinforced concrete slabs subjected, simultaneously, to thermal and mechanical loads. The analytical model based on the theory of linear elasticity consists to evaluate combined effects of thermal and mechanical loads on the transverse expansion of FRP bars. Parameters studied in this investigation are concrete cover thickness, bars diameter, mechanical load, and temperature variation. The thermal cycles were varied from -30 to +60°C .Comparisons between analytical and experimental results show that the transverse strains predicted from the proposed model are in good correlation with experimental results.

1 INTRODUCTION

The coefficient of thermal expansion (CTE) in the transverse direction of FRP bars is typically much higher than its longitudinal CTE. For glass fiber reinforced polymers (GFRP) bars, whilst the longitudinal CTE (LCTE) is similar to that of concrete, the transverse CTE (TCTE) is 3 to 8 times greater. Because of the difference between the transverse coefficients of thermal expansion of FRP bars and concrete, a radial pressure generated at the FRP bar/concrete interface induces tensile stresses within the concrete under the temperature increase. These tensile stresses may cause splitting cracks within concrete and eventually degradation of the member stiffness. As a consequence, important thermal strains take place just after appearance of the first micro cracking concrete which occurs when the thermal stress in the concrete around the GFRP bars, in different locations, reaches its tensile strength (*ft*). These thermal cracks may cause the degradation of the bond between GFRP bars and the surrounding concrete, and eventually, failure of the concrete cover if the confining action of concrete is not sufficient (Zaidi et al. 2006, EL-Zaroug et al. 2007).

Although, temperature effects on mechanical properties of FRP are recognized by all the documents reviewed, no guidance is given for the design of FRP reinforced structures for temperature (Elbadry et al. 2004). Hence, a better understanding of the thermal behavior of FRP reinforced concrete structures when subjected to large temperature variations is still required. This paper presents experimental and analytical studies on flexural behavior of concrete slabs reinforced with GFRP bars under the combined effect of mechanical loads and temperatures varied from -30 to +60°C. Comparisons between transverse thermal strains predicted from the proposed analytical model and those obtained from experimental tests are presented.

2 NOTATION

The following notations are used in this paper:

E_c : Young's modulus of concrete.
E_{ft} : Young's modulus of FRP bar in the transverse direction.
F_u: Ultimate load.
f_{c28} : Compressive concrete strength.
$r = b/a$: ratio of concrete cylinder radius "b" to FRP bar radius "a"
α_{ft} : Transverse coefficient of thermal expansion of FRP bars.
α_c: Coefficient of thermal expansion of concrete.
ε_{ft} : Circumferential strains in FRP bar at the interface of concrete/bar.
ε_{ct} : Circumferential strains in concrete at the interface of concrete/bar.
ε_{fl} : Longitudinal strain in the FRP bar due only to the mechanical loading.
ε_{cl} : Longitudinal strain in the tensile concrete due only to the mechanical loading.
ν_c : Poisson's ratio of concrete.
ν_{tt} : In-plane Poisson ratio of FRP bar (force and strains are both in transverse direction)
ν_{lt} : Major Poisson ratio of FRP bar (force is in the longitudinal direction and the strains in transverse direction.
ρ : Radius from the center of the concrete cylinder.
σ_{fl} : Tensile stress of reinforcement.
σ_{cl} : Tensile stress of concrete.

3 ANALYTICAL MODEL

The analytical model is established to analyze the combined effect of thermal and mechanical loads on the behavior of a concrete cylinder concentrically reinforced with FRP bar. The model studied is based on the following assumptions.

- A perfect bond between concrete and FRP bar.
- The behavior of concrete and FRP bars is linear elastic.
- The cross section of cylinder remains plane after deformation.
- Absence of transverse reinforcement to evaluate only the contribution of concrete cover to support the tensile stresses due to applied loads.

To determine thermal strains and stresses due to radial pressure P exerted by FRP bar on concrete cover under temperature increase ΔT, Rahman et al. (1995), have developed an analytical model based on the theory of elasticity of Timoshenko (1970) applied to a concrete cylinder axially reinforced with FRP bar and subject only to thermal loads. The expression of the radial pressure is given by:

$$P = \frac{\Delta_a}{\frac{a}{E_c}\left(\frac{r^2+1}{r^2-1}+\nu_c\right)+\frac{a}{E_{ft}}(1-\nu_{tt})} \qquad (1)$$

Where $\frac{\Delta_a}{a}$ is the differential deformation that occurs under no coupling between transverse deformations of concrete and the FRP bar.

Masmoudi et al. (2005) and Zaidi et al. (2008) have developed an analytical model based on the same theory. The expression of the radial pressure is given by:

$$P = \frac{\left(\alpha_{ft} - \alpha_c\right)\Delta T}{\frac{1}{E_c}\left(\frac{r^2+1}{r^2-1} + \nu_c\right) + \frac{1}{E_{ft}}(1-\nu_{tt})} \quad (2)$$

This model has been modified to take into account the axial force in FRP bar due to applied mechanical loads.

The circumferential strains in FRP bar (ε_{ft}) and in concrete (ε_{ct}) at the interface of concrete/bar ($\rho = a$) due to the radial pressure P, the temperature variation ΔT, and the mechanical load is given by the following equation (Figure 1):

$$\varepsilon_{ft}(a) = -\frac{1-\nu_{tt}}{E_{ft}} P + \alpha_{ft}.\Delta T - \nu_{lt}\varepsilon_{fl} \quad (3)$$

$$\varepsilon_{ct}(a) = \frac{P}{E_c}\left(\frac{r^2+1}{r^2-1} + \nu_c\right) + \alpha_c.\Delta T - \nu_c\varepsilon_{cl} \quad (4)$$

Where ε_{fl} and ε_{cl} are respectively the longitudinal strain in the FRP bar and in the tensile concrete due only to the mechanical loading.

The radial pressure P generated by the expansion of the FRP bar at the interface of concrete/bar is obtained from the compatibility equation of circumferential deformations ($\varepsilon_{ft} = \varepsilon_{ct}$). Equations 3 and 4 give:

$$P = \frac{\left(\alpha_{ft} - \alpha_c\right)\Delta T - \left(\nu_{lt}\varepsilon_{fl} - \nu_c\varepsilon_{cl}\right)}{\frac{1}{E_c}\left(\beta + \nu_c\right) + \frac{1}{E_{ft}}(1-\nu_{tt})} \quad (5)$$

Where: $\beta = \frac{r^2+1}{r^2-1}$

4 EXPERIMENTAL INVESTIGATION

4.1 Description and instrumentation of slabs

A total of six series of concrete slab specimens reinforced with GFRP bars were fabricated for this experimental program, each series is constituted by three slabs: SA, SB, and SC. The slabs had dimensions of 500 mm wide, (195, 200, and 215 mm) thick, 2500 mm total length and 2000 mm span between supports (Table 1). Three series of slabs were reinforced with six V-Rod glass FRP bars (GFRP) of 15.9 mm of diameter (bar #5), and three others were reinforced with

four V-Rod glass FRP bars of 19.1 mm of diameter (bar #6). The concrete covers used in this study (25, 30, and 45 mm) were selected according to ISIS-N°3-2007 recommendations of. The slab SA was subjected to both: temperature variations (from -30 to +60°C then to 30 freeze/thaw cycles) and mechanical loads which representing approximately 20% and then 30% of the ultimate load (F_u). The slab SB was subjected only to the temperature varied from -30 to +60°C then to 30 freeze/thaw cycles. The Slab SC is the control specimen and was stored under room temperature. The mechanical load applied on the slab was distributed on two transverse loading lines. Except the concrete cover thickness, diameter of bars, temperature variation, and mechanical loads, all other parameters were kept constant for all slab specimens.

Slabs were instrumented with strain gauges, thermocouples and LVDTs in order to measure deformations, temperatures, and deflections, respectively. Each slab was instrumented by six strain gauges installed on the main bar in both transverse and longitudinal directions. To measure the transverse and longitudinal strains of concrete, 3 strain gauges were placed on the lower tensioned surface of the slab during thermal tests. Then, 3 strain gauges were added on the upper compressed surface during the bending test. All strain gauges were installed on the mid-span. To measure the deflection and crack opening, two LVDTs and two sensor cracks were placed at mid-span and at 3/8 of the slab span.

4.2 Test Procedure

Concrete slab specimens SA and SB were subjected to temperatures varied from +20°C to -30°C then from -30°C to +60°C using the thermal room shown in Figure 2. Once the temperature had stabilized in the concrete and GFRP bars for each increment, all temperature and strain gauge readings were recorded. The temperature was increased by increments of 10 °C, each increment required 10 to 16 hours to reach a stable and uniform temperature distribution throughout the slab. The samples were subsequently examined visually to note any cracks. In addition to the thermal load, the slab SA was submitted to a mechanical load which represent approximately 20% of the ultimate load (F_u) (for the 1st thermal loading cycle) and 30% F_u (for the 2nd thermal loading cycle). The total loads are nearly 40 kN for the 1st thermal loading cycle and 60 kN for the 2nd thermal loading cycle. When the mechanical strains were stabilized, all the strains were recorded and then put to zero in order to present the results in terms of thermal strains alone. The second step was to submit the slabs SA and SB to 30 freeze/thaw cycles from -30 °C to +30 °C. The slab SA was kept under the same mechanical load of 20%. At the end of this step, the first step was repeated again with a mechanical load of 30% instead 20%. At the end of thermal cycles, the three slabs SA, SB, and SC, were subjected to four-points bending test up to failure. In this paper, the only 1st thermal loading cycle results of slabs SA are presented.

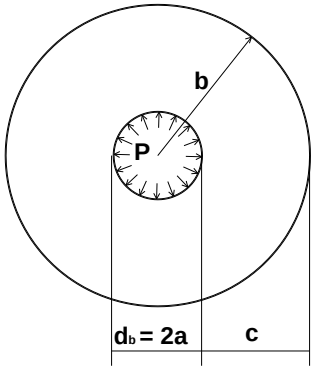

Figure 1. Axisymetric model of a concrete cylinder concentrically reinforced with FRP bar.

Figure 2. The environmental room including the four point flexural setup, slabs SA and SB.

Table 1. Mechanical properties of concrete used.

Slabs	Concrete cover (mm)	Longitudinal modulus of elasticity, E_C (GPa)	Compression strength (MPa)	Tensile strength (MPa)
SA195.25.16	25	26.17±0.4	33.83±1	1.94±0.04
SA200.30.16	30	24.80±0.8	30.39±2	2.58±0.04
SA215.45.16	45	26.17±0.4	33.83±1	1.94±0.04
SA195.25.19	25	26.53±0.3	34.77±0.7	2.77±0.15
SA200.30.19	30	27.34±0.7	36.93±2	2.92±0.25
SA215.45.19	45	27.34±0.7	36.93±2	2.92±0.25

Table 2. Mechanical and thermal properties of GFRP reinforcing bars.

Bars diameter (mm)	Longitudinal Modulus of elasticity, E_{fl} (GPa)	Transverse modulus of elasticity, E_{ft} (GPa)	Poisson's ratio in the longitudinal direction, ν_{lt}	Poisson's ratio in the transverse direction, ν_{tt}
15.9	47.0±0.3	7.75	0.28±0.005	0.38
19.1	52.2±1.2	7.87	0.28±0.008	0.38

Ultimate tensile strength (MPa)	Guarantee tensile strength (MPa)	Ultimate tensile strain (%)	TCTE* (α_{ft}) [x10^{-6}] /°C	LCTE‡ (α_{fl}) [x10^{-6}] /°C
700±24	683	1.50±0.06	27.35±0.35	6.81±0.9
691±7	656	1.33±0.03	22.45±0.31	6.61±0.1

* TCTE: Transverse Coefficient of Thermal Expansion.
‡ LCTE: Longitudinal Coefficient of Thermal Expansion.

4.3 Materials

4.3.1 Concrete

For each slab, six standard concrete cylinders of 150 x 300 mm were cast and cured with water for 28 days at room temperature under the same conditions as the slab specimens. Cylinders were tested to evaluate the compression and tensile strengths of concrete at 28 days and immediately before slab specimen tests. The tensile strength was determined by the splitting test. The modulus of elasticity is calculated as recommended by the code CAN/CSA-S806-02. Poisson's ratio and coefficient of thermal expansion are assumed equal to 0.17 and 11.7x10^{-6} /°C respectively, as an ordinary concrete. The mechanical properties of concrete are presented in Table 1.

4.3.2 Bars

The mechanical and thermal properties of V-Rod GFRP bars used in this study are presented in Table 2. The modulus of elasticity is calculated as recommended by the code ACI 440.3R-04.

The coefficients of thermal expansion were measured by the Thermo Mechanical Analysis (TMA) test. The other properties are the manufacturer's specified values.

5 RESULTS AND ANALYSIS

Figures 3 to 8 show transverse thermal strains at the concrete/FRP bar interface as a function of temperature variation (ΔT) of slabs SA after the 1st thermal loading cycle (for a temperature varied from -30°C to +60°C and an applied mechanical load of 20% F_u).

Figures 3 to 7 compare experimental results with analytical predictions given by Eq. 3. It is observed that experimental results are widely higher than those obtained from the analytical model. This divergence is probably due to the development of circumferential cracks around FRP bars due to tensile stresses caused by shrinkage that has sustained the bar at low temperatures. Then, it added to these cracks, radial cracks caused by the thermal expansion of FRP bars due to the temperature increase. These cracks were not taken into account in the assumptions of the analytical model based on the theory of elasticity.

To determine transverse strains of FRP bars, the analytical model (Eq. 3) was modified to fit the experimental results obtained from FRP-reinforced concrete slabs tested under a temperature varied from -30°C to + 60°C applied simultaneously with a mechanical loading of 20% of the ultimate load of slabs. The proposed model is given by:

$$\left.\begin{aligned} \varepsilon_{ft} &= \frac{r\,\alpha_{ft}\,\Delta T}{0.4\,\sqrt{f_{c28}}\,Ln\,r} - 0.1\,\nu_{lt}\,\varepsilon_{fl} && for\ \Delta T > 0 \\ \varepsilon_{ft} &= 0.4\,\left(c/d\right)\alpha_{ft}\,\Delta T - 0.1\,\nu_{lt}\,\varepsilon_{fl} && for\ \Delta T \le 0 \end{aligned}\right\} \quad (6)$$

Figures 3 to 7 show that transverse strains predicted from the proposed model are in good agreement with experimental results. It should be noted that this model are only valid for materials used in this study.

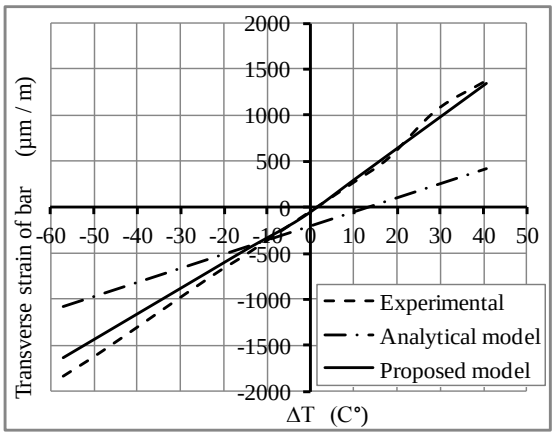

Figure 3. Transverse strain of FRP bars of slab SA.25.16 – Experimental results and analytical results comparison.

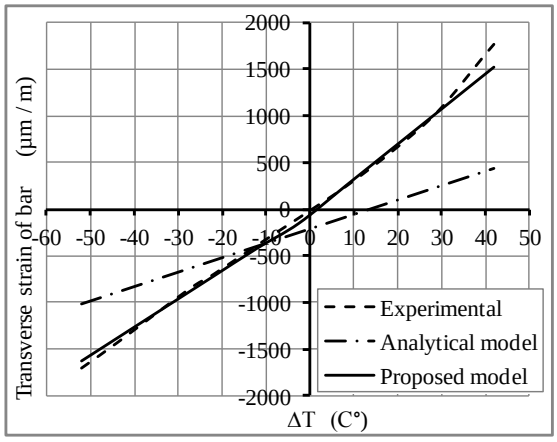

Figure 4. Transverse strain of FRP bars of slab SA.30.16 – Experimental results and analytical results comparison.

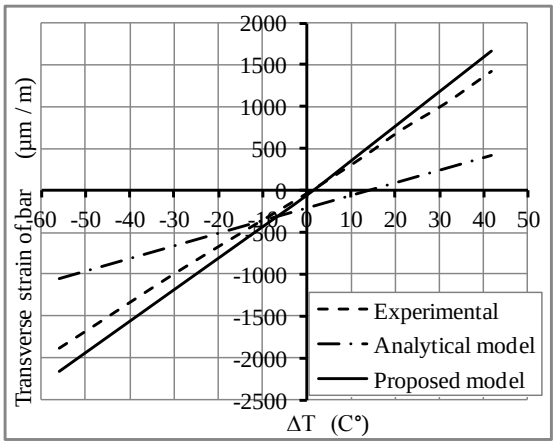

Figure 5. Transverse strain of FRP bars of slab SA.45.16 – Experimental results and analytical results comparison.

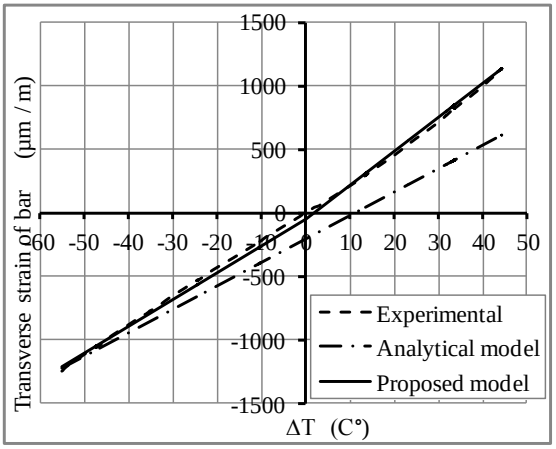

Figure 6. Transverse strain of FRP bars of slab SA.25.19 – Experimental results and analytical results comparison.

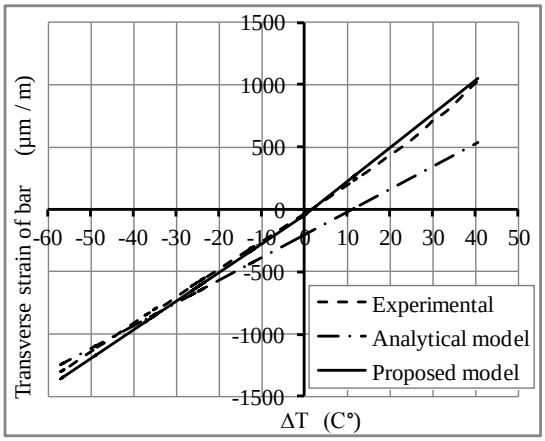

Figure 7. Transverse strain of FRP bars of slab SA.30.19 – Experimental results and analytical results comparison.

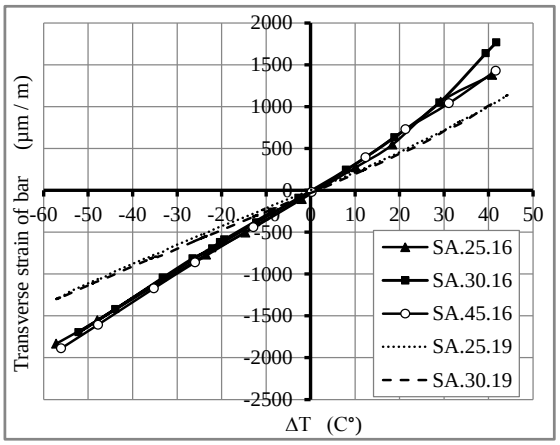

Figure 8. Experimental transverse strain of FRP bars for concrete slabs SA having different concrete cover and FRP bars diameter.

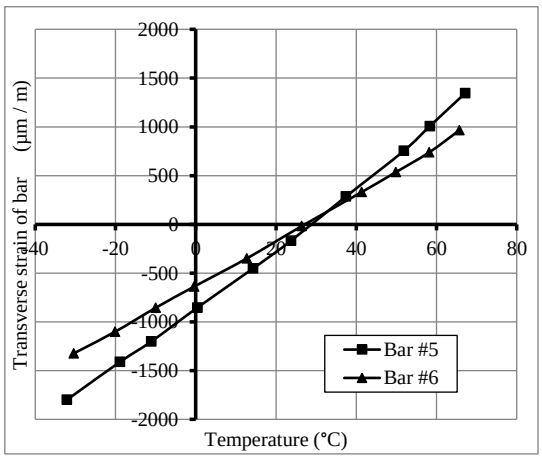

Figure 9. Transverse strain of isolated FRP bars subjected simultaneously to thermal and mechanical load.

Figure 10. Conditioned tensile test setup of GFRP bars.

Figure 8 compares experimental results of slabs SA having different concrete cover thickness (25, 30, and 45 mm) and different bar diameter (# 5and # 6). This figure shows that the variation of concrete cover thickness does not affect transverse thermal strains of FRP bars. However, the increase of FRP bar diameter conducts to the decrease of these strains. This is due to the lower value of the transverse coefficient of thermal expansion of FRP bars # 6 is compared to that of FRP bars # 5 (Table 2). It should be noted that the transverse expansion of FRP bars is governed by the resin, while the longitudinal expansion is governed by the fiber (Vogel et al. 2004). This is proved also by the experimental results obtained from isolated GFRP bars (# 5and # 6) tested under the same conditions of the tested slabs (Figure 9 and 10).

6 CONCLUSIONS

The analysis of analytical and experimental results allows to draw the following conclusions:

- The concrete cover thickness variation has no big effect on transverse thermal strains at FRP bar/concrete interface, for temperature varied from -30°C to +60°C.
- The transverse strains, at concrete/FRP bars interface of concrete slab under thermal and mechanical loads, predicted from the analytical model are greater than those obtained from experimental tests. This is due to the presence of cracks produced within concrete at the interface which is not considered in the linear analytical model based on the theory of elasticity.
- The transverse strains, at FRP bars/concrete interface, predicted from the proposed model, are in good agreement with experimental results obtained from GFRP bars-reinforced concrete slabs under the combined thermal load (from -30 to +60°C) and mechanical load (20% of the ultimate load of slabs).

Acknowledgments

The research reported in this paper was carried out at the University of Sherbrooke. Thanks to the personnel of the laboratory of the civil engineering department of the University of the Sherbrooke. Also, Special thanks to "Le Ministère de l'Enseignement supérieur et de la recherche scientifique" of Algeria for the PhD scholarship granted to Bellakehal (PhD candidate). The research reported in this paper was partially sponsored by the Natural Sciences and Engineering Research Council of Canada (NSERC). The authors also acknowledge the contribution of the Canadian Foundation for Innovation (CFI) for the infrastructure used to conduct testing. Special thanks to the manufacturer (Pultrall Inc., QC, Canada) for providing FRP bars. The opinion and analysis presented in this paper are those of the authors.

7 REFERENCES

Elbadry, M, Elzaroug, O. 2004. Control of cracking due to temperature in structural concrete reinforced with CFRP bars. *Composite Structures*, 64: 37-45

EL-Zaroug, O, Forth, J, Ye, J, Beeby, A. 2007. Flexural performance of concrete slabs reinforced with GFRP and subjected to different thermal histories. *FRPRCS-8,* Greece, pp. 1-10.

Masmoudi, R, Zaidi, A, and Gérard, P. 2005. Transverse thermal expansion of FRP bars embedded in concrete. *Journal of composites For construction*, 9(5): 377-387.

Rahman, HA, Kingsley, CY, and Taylor, DA. 1995. Thermal stress in FRP reinforced concrete. *Proceeding of Annual Conference of the Canadian Society for Civil Engineering*, Ottawa, pp. 605-614.

Timoshenko, SP, and Goodier, JN. 1970. *Theory of elasticity*. Mc-Graw-Hill, New York, USA.

Vogel, H, Svecova, D. 2004. Effect of temperature on concrete cover of FRP prestressed elements. *Proceeding of Advanced composite materials in bridges and structures (IV ACMBS)*, Alberta, pp. 1-8.

Zaidi, A, and Masmoudi, R. 2006. Thermal effect on FRP-reinforced concrete slabs. *1st International Structural Specialty Conference*. CSCE. Alberta, ST-036 : 1-10.

Zaidi, A, Masmoudi, R. 2008. Thermal effect on fiber reinforced polymer reinforced concrete slabs. *Canadian Journal of Civil Engineering*, pp: 312-320.